

OSTEOPOROSIS AND ANTERIOR FEMORAL NOTCHING IN PERIPROSTHETIC SUPRACONDYLAR FEMORAL FRACTURES

A BIOMECHANICAL ANALYSIS

BY MAJOR SCOTT B. SHAWEN, MD, MAJOR PHILIP J. BELMONT JR., MD, LIEUTENANT COLONEL(P) WILLIAM R. KLEMME, MD, L.D. TIMMIE TOPOLESKI, PhD, LIEUTENANT COLONEL JOHN S. XENOS, MD, AND MAJOR JOSEPH R. ORCHOWSKI, MD

Investigation performed at Walter Reed Army Medical Center, Washington, DC, and University of Maryland, Baltimore County, Maryland

Background: This biomechanical study was designed to evaluate the predictive ability of dual-energy x-ray absorptiometry, cortical bone geometry as determined with computed tomography, and radiography in the assessment of torsional load to failure in femora with and without notching.

Methods: Thirteen matched pairs of cadaveric femora were randomized into two groups: a notched group, which consisted of femora with a 3-mm anterior cortical defect, and an unnotched group of controls. Each pair then underwent torsional load to failure. The ability of a number of measures to predict femoral torsional load to failure was assessed with use of regression analysis. These measures included dual-energy x-ray absorptiometry scans of the proximal and the distal part of the femur, geometric measures of both anterior and posterior cortical thickness as well as the polar moment of inertia of the distal part of the femur as calculated on computed tomography scans, and the Singh osteoporosis index as determined on radiographs.

Results: The torsional load to failure averaged 98.9 N-m for the notched femora and 143.9 N-m for the controls; the difference was significant ($p < 0.01$). Although several variables correlated with torsional load to failure, distal femoral bone-mineral density demonstrated the highest significant correlation ($r = 0.85$; $p < 0.001$). Moreover, multiple regression analysis showed that a combination of distal femoral bone-mineral density and polar moment of inertia calculated with the posterior cortical thickness (adjusted $r^2 = 0.79$; $p < 0.001$) had the strongest prediction of torsional load to failure in the notched group. The addition of other measures of cortical bone geometry, proximal femoral bone-mineral density, or radiographic evidence of osteopenia did not significantly increase the model's predictive ability.

Conclusions: Femoral notching significantly decreases distal femoral torsional load to failure and is best predicted by a combination of the measures of distal femoral bone-mineral density and polar moment of inertia. Together, these values account for the amount of bone mass present and the stability provided by the cortical shell architecture.

Clinical Relevance: Femoral notching during total knee arthroplasty decreases distal femoral torsional load to failure. By examination of femoral bone density and distal femoral geometry, the relative decrease in torsional load to failure can be predicted and appropriate precautions taken.

Periprosthetic supracondylar femoral fractures are an uncommon complication following total knee arthroplasty, with a reported prevalence of 0.30% to 4.8%¹⁻⁷. Predisposing factors for these fractures include osteopenia, femoral

notching, chronic steroid use, rheumatoid arthritis, arthrofibrosis, revision total knee arthroplasty, and severe neurologic disorders^{1-3,5-18}. Among the numerous factors associated with these fractures, osteopenia or conditions that induce osteopenia, such as rheumatoid arthritis and prolonged steroid use, and femoral notching are implicated most often^{1,5,10,13,15,16,19}.

The prevalence of notching of the anterior femoral cortex in total knee arthroplasty has been reported to range from



A commentary is available with the electronic versions of this article, on our web site (www.jbjs.org) and on our quarterly CD-ROM (call our subscription department, at 781-449-9780, to order the CD-ROM).

3.5% to 26.9%^{1,3,6}. Importantly, periprosthetic femoral fractures are not always associated with femoral notching or osteopenia. The prevalence of anterior femoral notching associated with periprosthetic femoral fractures has been reported to range from 7% to 50%^{1,3,5,6,10,13,15,16,19}, and the prevalence of radiographic evidence of osteopenia associated with such fractures, from 49% to 100%^{1,5,10,13,15}.

Femoral bone strength can be predicted by a number of imaging modalities. These include measurement of bone-mineral density with use of dual-energy x-ray absorptiometry, assessment of cortical bone geometry with use of computed tomography, and determination of the Singh index with use of plain radiography. However, these studies have been principally applied to the proximal aspect of the femur²⁰⁻²⁵. To our knowledge, no reports have detailed the predictive value of these studies as indicators of distal femoral torsional load to failure.

The purposes of this study were (1) to examine the effects of anterior femoral notching on distal femoral torsional load to failure and (2) to assess the utility of densitometric, cortical geometric, and radiographic measures in predicting the torsional load to failure of distal femoral specimens with and without anterior femoral notching.

Materials and Methods

Biomechanical analysis was conducted on thirteen matched pairs of fresh-frozen cadaveric femora that were obtained from donors without a history of metastatic disease or metabolic bone disease. The average age of the individuals at the time of death was 76.5 years (range, fifty-nine to eighty years). Nine were male and four were female. All soft tissues were removed at the time of retrieval, and the specimens were immediately frozen at -20°C and stored until testing. Prior to testing, all specimens were thawed overnight under refrigerated conditions.

On the day of testing, dual-energy x-ray absorptiometry scans of the proximal and the distal aspect of the femur were performed, with use of a standard protocol, on a densitometer (QDR-2000; Hologic, Bedford, Massachusetts). The bone-mineral density values in the proximal part of the femur were obtained from the Ward triangle at the base of the femoral neck. The distal femoral metaphyseal bone-mineral density was measured in each specimen 2 cm proximal to the femoral condyles in an area of approximately 20 cm^2 .

The paired femora were then randomized into one of two groups: a notched group, which received an anterior cortical defect, and an unnotched control group. All femora underwent mock total knee arthroplasty, consisting of distal femoral cuts with use of posterior-cruciate-retaining cutting jigs (DePuy, a Johnson and Johnson Company, Warsaw, Indiana). In the notched group, the sizing jig was moved 3 mm posteriorly on the femora, prior to drilling for the cutting block, to create a full-thickness anterior cortical defect, or notch, measuring approximately 3-mm in depth. This cut was performed to the length of the standard oscillating saw-blade over the cutting block (approximately 5 cm). No attempt was made to smooth the transition from the notch to the anterior femoral cortex.

Distal and posterior cuts, excluding the chamfer cuts, were performed as dictated by the established protocol.

Anteroposterior and lateral radiographs were made prior to biomechanical testing. Femora were excluded if there were any osseous lesions or evidence of metabolic bone disease. Computed tomography (Advantage 2X High Speed scanner; General Electric, Milwaukee, Wisconsin) of the distal aspect of each femur was performed to evaluate the anterior, posterior, and lateral cortical thickness as well as to measure the transverse and sagittal femoral diameter with use of digital calipers. Each pair of femora was scanned side by side, and values were obtained just proximal to the femoral cut in the notched femora and at the same scanned level for the unnotched controls. Those values were then used to calculate the polar moments of inertia for each specimen with use of the equation established by Culp et al.¹³. Since the cortical thickness was, on the average, greater posteriorly than anteriorly, calculations of the polar moment of inertia were performed with use of the values for both anterior and posterior cortical thickness. Additionally, both radiographs and computed tomography scans were used to confirm that the anterior cortex was intact in the control group and to measure and verify the anterior cortical defect in the notched group.

With use of the method of Singh et al.²⁶, radiographs of the paired femora were evaluated independently by three orthopaedic surgeons for evidence of bone-mineral loss. Each femur was graded from 1 to 6, with 1 signifying the lowest bone-mineral density and 6, the highest. The grades from all observers were then averaged for each femur.

The femora were transected in the diaphyseal region at a point determined to be 60% of the total femoral length measured from the lateral femoral condyle to the greater trochanter. Specimens were embedded proximally and distally in fast-curing polyester casting resin and were further stabilized with reinforcing screws. Care was taken to ensure that the distal part of the femur was completely embedded in 3 cm of polyester casting resin, covering both of the femoral condyles and the epicondyles in all specimens. In the notched group, the resin did not cover any portion of the femur proximal to the notch. Torsional testing was performed on each specimen at a constant rate of $1^{\circ}/\text{sec}$ in a servohydraulic test frame (MTS Systems, Eden Prairie, Minnesota) until failure occurred. A torsional load was applied to the specimen until failure because this is thought to be the primary mechanism in the production of periprosthetic femoral fractures²⁷. In addition, the reduction in torsional load to failure after anterior femoral notching is known to exceed the strength reduction in straight bending by a factor of two²⁸. Finally, load displacement curves were generated, and the torsional load to failure was recorded in N-m at a rate of 10 Hz. The fracture pattern and fracture location were recorded for both the notched and control groups.

Statistical Methods

Seven potential variables were available to predict distal femoral torsional load to failure, and these were recorded with use

TABLE I Regression Variables		
Dual-Energy X-ray Absorptiometry Regions	Cortical Values Calculated with Use of Computed Tomography*	Radiographic Evaluation
Ward triangle (proximal part of femur)	Anterior cortical thickness Posterior cortical thickness	Singh index
Distal part of femur	Anterior polar moment of inertia Posterior polar moment of inertia	

*The polar moment of inertia was calculated with use of anterior or posterior cortical thickness.

of dual-energy x-ray absorptiometry, computed tomography geometric measurements, or radiographic evaluation, as applicable (Table I). Single-variable linear regression analysis was used to determine the correlation coefficients (r) and the significance of each regressor for both the notched and control groups. A full model containing all independent variables was then constructed. The model was examined for multicol-

linearity among the independent variables within each group by reviewing the correlations among the independent variables, examining the variance inflation factors and regression coefficient estimates, and computing the principal components of the independent variables. The models were then redefined by deleting correlated ($r > 0.80$) independent variables within the same group to minimize the effects of multicollinearity.

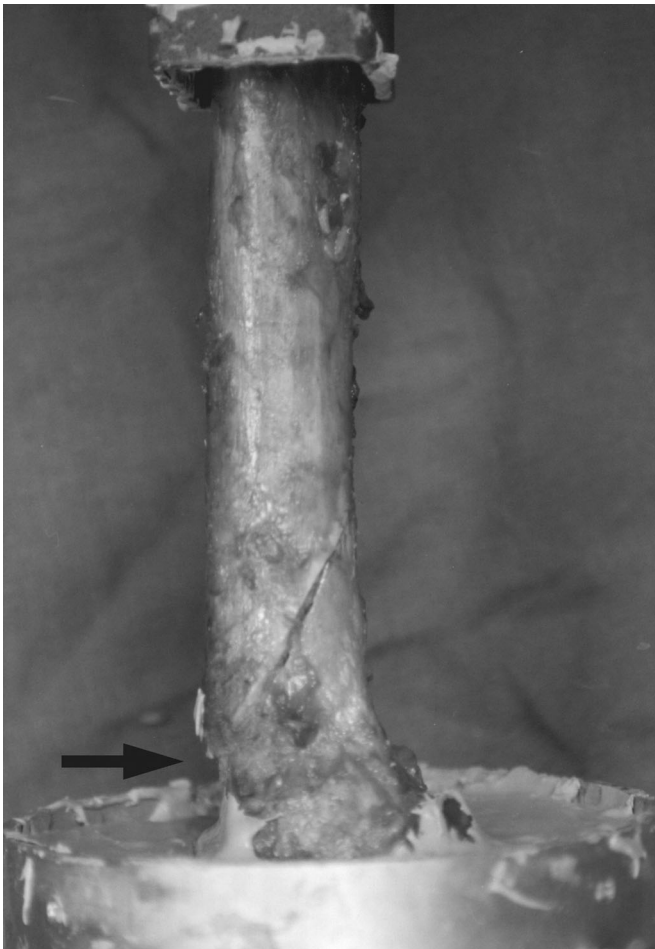


Fig. 1-A

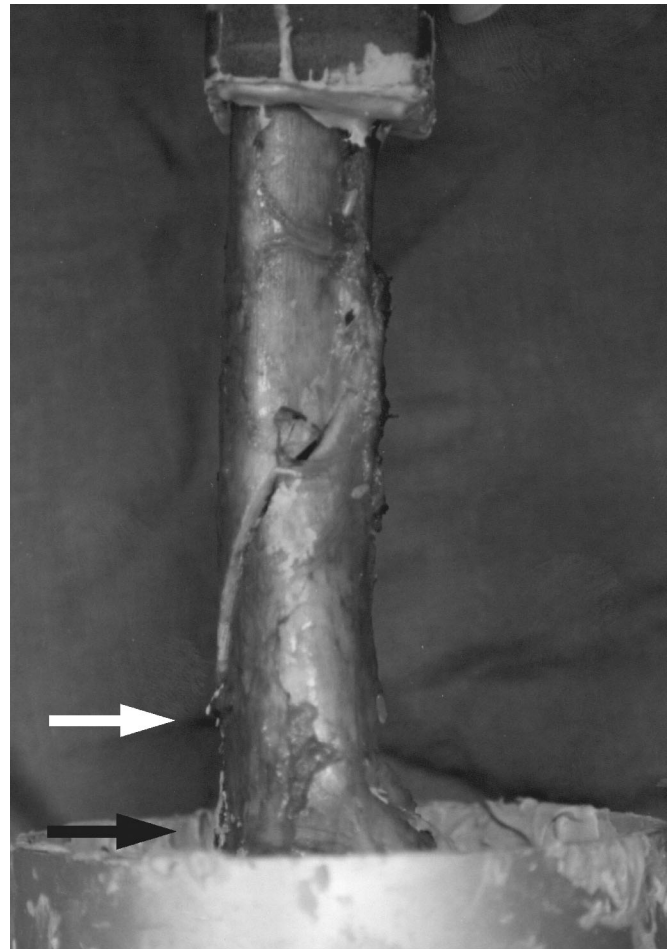
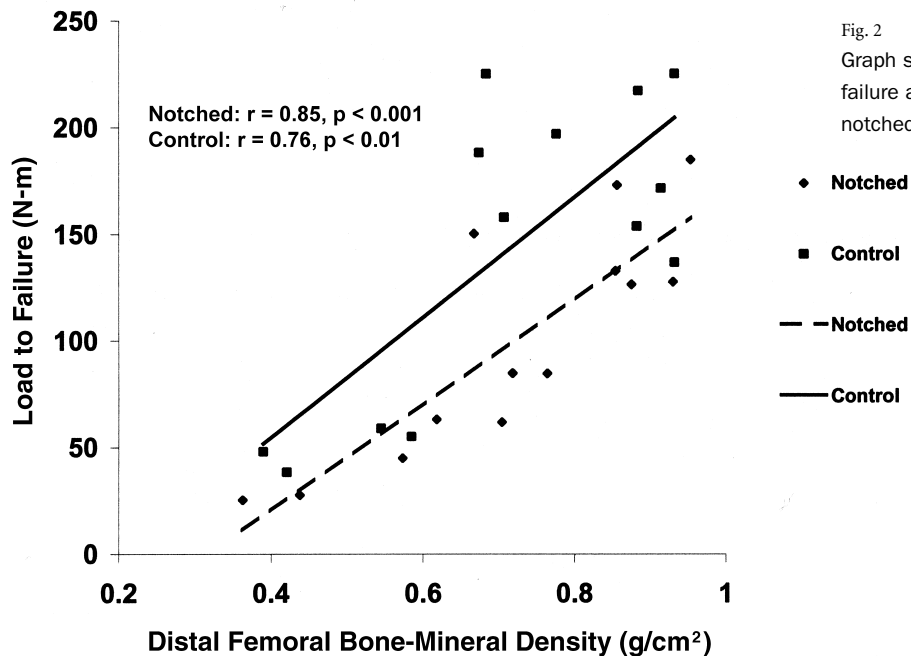


Fig. 1-B

Fracture lines demonstrating extension into the anterior bone cut in a notched femur (Fig. 1-A) and spiral metaphyseal involvement above the bone cut in a control femur (Fig. 1-B). Black arrows demonstrate the proximal extent of the bone cuts. The white arrow demonstrates the distal extent of the fracture line.



The remaining independent variables were then analyzed with use of stepwise forward and backward as well as best-fit subsets regression with use of the following criteria: C_p to avoid bias due to the number of variables*, adjusted r^2 , and F statistic for incremental change in r^2 . Models were then selected when the number of independent variables plus one was approximately equal to C_p , the adjusted r^2 was maximized, and significance was achieved ($F > 4.0$; $p < 0.05$). The difference between the notched and control specimens with respect to the torsional load to failure was compared, with use of the paired t test. The Mann-Whitney rank-sum test was performed to compare the values for the anterior and the posterior polar moment of inertia. Single-variable linear regression was also used to determine the correlation between and within the data from dual-energy x-ray absorptiometry and the Singh index. All statistical analysis was performed with use of Sigma Stat software (version 1.0; Jandel Scientific, San Rafael, California).

Results

All thirteen pairs of femora were available for testing and analysis. The descriptive statistics of the different measures of femoral bone strength obtained from dual-energy x-ray absorptiometry, computed tomography, and plain radiographs as well as the corresponding torsional load to failure and fracture location for both the notched and control specimens are presented in the Appendix. A significant correlation ($r = 0.79$;

$p = 0.01$) was found between the proximal and the distal femoral bone-mineral density. Additionally, the Singh index values had a significant correlation with proximal femoral bone-mineral density ($r = 0.52$; $p = 0.01$) and distal femoral bone-mineral density ($r = 0.52$; $p = 0.01$).

The torsional load to failure was an average of 98.9 N-m for the notched group and 143.9 N-m for the control group of femora; the difference was significant ($p < 0.01$). Fracture lines in the notched femora extended into the anterior notch in all thirteen femora, whereas no extension into the bone cuts was noted in any of the thirteen femora in the control group (Figs. 1-A and 1-B).

With use of the data from the femoral torsional load-to-failure testing and those obtained from dual-energy x-ray absorptiometry, computed tomography scans, and radiographs of the femora, single linear regression was performed to determine the correlation coefficients (r) and the significance of each regressor (see Appendix). Examination of the predictive ability of the different measurements made with dual-energy x-ray absorptiometry in the notched group demonstrated that distal femoral bone-mineral density had the highest significant correlation with torsional load to failure of any regressor ($r = 0.85$; $p < 0.001$) (Fig. 2). In contrast, dual-energy x-ray absorptiometry in the Ward triangle had the highest significant correlation with torsional load to failure of any regressor ($r = 0.80$; $p < 0.001$) in the control group. Examination of the predictive ability of the geometric measurement data obtained from computed tomography scanning of the distal part of the femur in the notched group demonstrated that the posterior polar moment of inertia correlated most strongly with torsional load to failure ($r = 0.70$; $p = 0.008$) (Fig. 3). Conversely, in the control group, the anterior polar moment of inertia correlated most strongly with torsional load to failure ($r =$

*During best-fit analysis, C_p (Mallows C_p) is a gauge of the bias introduced into the estimate of the dependent variable when independent variables are omitted from the regression equation. The optimal value of C_p is equal to the number of parameters (the independent variables used in the subset plus the constant), or $C_p = p + k + 1$, where p is the number of parameters and k is the number of independent variables. The closer the value of C_p is to the number of parameters, the less likely a relevant variable was omitted. Subsets with low orders that also have C_p values close to $k + 1$ are good candidates for the best subset of variables.

0.63; $p = 0.021$). Although the other geometric measures of anterior and posterior cortical thickness of the distal part of the femur correlated with torsional load to failure in the notched group, these correlations were considerably weaker ($r \leq 0.51$; $0.076 < p < 0.095$). The Singh osteoporosis index data had the weakest correlation with torsional load to failure in the notched group ($r = 0.39$; $p = 0.216$) but demonstrated a much stronger correlation with torsional load to failure in the control group ($r = 0.70$; $p = 0.012$).

In the notched group, multiple regression analyses showed that the different imaging and geometric measures obtained from dual-energy x-ray absorptiometry and computed tomography, when taken together, were better predictors of torsional load to failure than were individual measures (Table II). Forward, backward, stepwise, and maximum adjusted correlation techniques performed with use of all predictive variables resulted in one significant model of torsional load to failure for the notched group. Specifically, a linear combination of distal femoral bone-mineral density and posterior polar moment of inertia provided the best multiple linear regression model for the notched group (adjusted $r^2 = 0.79$; $p < 0.001$). In the presence of these two variables, none of the other individual variables, which correlated with load to failure as individual regressors, added predictive ability to the model for the notched group. Similarly, the values according to the Singh index did not provide a significant improvement in the prediction of torsional load to failure in the presence of distal femoral bone-mineral density and posterior polar moment of inertia in the notched group.

In the control group, a linear combination of distal femoral bone-mineral density and anterior polar moment of inertia provided the best multiple linear regression model (adjusted $r^2 = 0.65$; $p = 0.002$) for predicting torsional load to failure. The addition of other cortical geometric measures of the distal part of the femur or measures of bone density as determined by dual-energy x-ray absorptiometry or radiographs did not increase the model's predictive ability in the presence of these measures.

Discussion

Femoral notching and osteopenia are thought to be the two primary variables that are responsible for the occurrence of periprosthetic supracondylar femoral fractures. In our study, torsional testing of paired femora after mock total knee replacement demonstrated a 31% decrease in distal femoral torsional load to failure after notching of the anterior femoral cortex ($p < 0.01$). These findings are similar to the 39% decrease in torsional load to failure reported by Lesh et al.²⁸, and they serve to corroborate the theoretical 29% decrease in distal femoral torsional strength after 3 mm of anterior femoral notching, which was predicted by Culp et al.¹³. In contrast to the study by Lesh et al.²⁸, who reported that even femora without notching had a spiral fracture that had originated along the anterior aspect of the bone cuts, the current study found that torsional load to failure in the control group resulted in spiral meta-diaphyseal fracture patterns, which did not extend at all into the bone cuts in any of the thirteen specimens.

The testing apparatus was designed to limit variability between specimens. The application of a torsional load on the tibia through intact ligaments would closely mimic the clinical origin of supracondylar fractures, but it may have introduced variability into the model. The ligament strength or knee position when load was applied would be difficult to control between specimens.

Although the bone strength of the distal part of the femur cannot be directly assessed, two of its major components, bone density and cortical bone geometry, are measurable by non-invasive methods. Bone-mineral density, measured by dual-energy x-ray absorptiometry, is often used to assess fracture risk in vivo²². This assessment method is based on the assumption that bone-mineral content is the primary determinant of whole-bone strength. Geometric parameters, which are often made from computed tomography measurements, delineate the spatial distribution of tissues within the cortical and cancellous bone and have been used as predictors of whole-bone strength. The single geometric parameter that has been most often cited

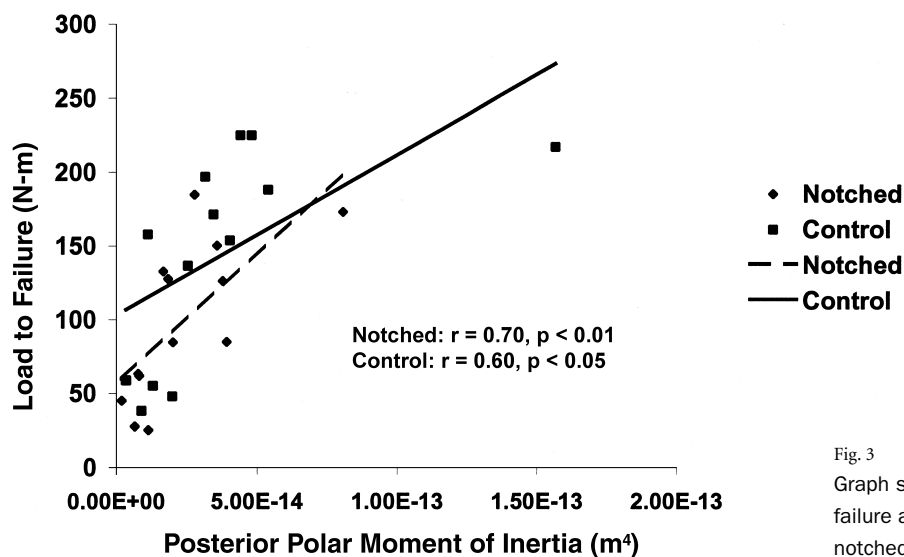


Fig. 3

Graph showing the correlation between torsional load to failure and posterior polar moment of inertia for the notched and control specimens.

TABLE II Best Multiple-Regression Models for Prediction of Femoral Torsional Load to Failure

Measure*	Notched Group	Control Group
Distal femoral bone-mineral density and anterior polar moment of inertia	r = 0.908 adjusted r ² = 0.790 p < 0.001	r = 0.840 adjusted r ² = 0.647 p = 0.002
Distal femoral bone-mineral density and posterior polar moment of inertia	r = 0.909 adjusted r ² = 0.791 p < 0.001	r = 0.812 adjusted r ² = 0.591 p = 0.005
Ward triangle bone-mineral density and anterior polar moment of inertia	r = 0.811 adjusted r ² = 0.589 p = 0.005	r = 0.829 adjusted r ² = 0.625 p = 0.003
Ward triangle bone-mineral density and posterior polar moment of inertia	r = 0.842 adjusted r ² = 0.651 p = 0.002	r = 0.814 adjusted r ² = 0.596 p = 0.004

*The polar moment of inertia was calculated with use of anterior or posterior cortical thickness.


as a predictor of whole-bone strength is the polar moment of inertia^{13,21,29}. In torsion, the polar moment of inertia relates the applied torque to the maximum stress that arises within the cross section. Calculation of the Singh index of the proximal part of the femur was proposed as a clinically applicable method to evaluate osteoporosis with use of plain radiographs²⁶. This method, however, relies on subjective observations of the qualitative change in the trabecular pattern of cancellous bone in the proximal part of the femur that are converted to a score by the observer; therefore, at best, it produces results with uneven reproducibility or reliability^{25,30-32}. No consensus has been reached with regard to which predictors of whole-bone strength in the distal part of the femur are most accurate.

Our study showed that distal femoral bone-mineral density derived from dual-energy x-ray absorptiometry ($r = 0.85$; $p < 0.001$) had the greatest predictive value for torsional load to failure in notched femora. Multiple regression analyses identified a combination of distal femoral bone-mineral density and posterior polar moment of inertia as the strongest predictive model of femoral torsional load to failure in the notched group (adjusted $r^2 = 0.79$; $p < 0.001$). The use of these two variables as predictors of load to failure makes anatomical sense because one accounts for the substantial stability provided by the cortical shell architecture and the other accounts for the amount of bone-mineral density. The combination of the two variables provides greater predictive ability with regard to the risk of periprosthetic femoral fracture than that provided when either variable is used individually. This finding is particularly relevant in the evaluation of the age-related changes associated with osteoporosis in the distal part of the femur, as Peacock et al.³¹ reported that, in addition to the decrease in bone-mineral density seen in both sexes, women exhibit an increase in the width of the medullary canal and a decrease in the polar moment of inertia. Conversely, in the control group, a linear combination of distal femoral bone-mineral density and anterior polar moment of inertia provided the best multiple linear regression model (adjusted $r^2 = 0.65$; $p = 0.002$).

In any statistical analysis, failure to realize a significant correlation may result from a small sample size, a narrow domain of the independent variable, the presence of large measurement error, or many closely related regressors. Accordingly, in the present study, each regressor was analyzed separately and each group was analyzed individually in addition to an analysis of all regressors. To ensure a wide domain of each independent variable, the femora were obtained from a large enough sample of donors to ensure substantial variations in bone-mineral density, geometric measures of cortical bone, and Singh index data. To further reduce the possibility of statistical error, four model-generation techniques and three inclusion criteria were used. In both the control and notched groups, the analyses generated a single model with only two independent variables that showed significant predictive ability, thereby suggesting that the results are valid. Variables that do not correlate or that show weak correlation are not dismissed as being unrelated to torsional load to failure; however, the importance of their predictive ability, if any, is small compared with that of the variables that were identified as significant.

In conclusion, 3 mm of anterior femoral notching decreased the torsional load to failure of the distal part of the femur by 31%. The major determinants of distal femoral load to failure were found to be the amount of bone mass present, as determined from local bone-mineral density, and distal femoral cortical bone geometry, as calculated with the posterior polar moment of inertia. This combination of variables was shown to be the most useful predictor of the in vitro torsional load to failure of notched femora. Although these variables are interrelated, they provide significantly greater prediction of torsional load to failure in notched femora when they are used together than when they are used individually.

Appendix

 Tables showing the descriptive statistics of the notched and control specimens and the best single regression variables for prediction of femoral torsional load to failure are

available with the electronic versions of this article, on our web site at www.jbjs.org (go to the article citation and click on "Supplementary Material") and on our quarterly CD-ROM (call our subscription department, at 781-449-9780, to order the CD-ROM). ■

Major Scott B. Shawen, MD
Major Philip J. Belmont Jr., MD
Lieutenant Colonel(P) William R. Klemme, MD
Lieutenant Colonel John S. Xenos, MD
Major Joseph R. Orchowski, MD
Orthopaedic Surgery Service, Department of Orthopaedics and Rehabilitation, Walter Reed Army Medical Center, Washington, DC 20307. E-mail address for S.B. Shawen: sshawen@usa.net

L.D. Timmie Topoleski, PhD
Department of Mechanical Engineering, University of Maryland, Baltimore County, Baltimore, MD 21250

The opinions or assertions contained herein are the private views of the authors and are not to be construed as official or as reflecting the views of the Department of the Army or the Department of Defense. All authors are employees of the United States government. This work was prepared as part of their official duties and, as such, there is no copyright to be transferred. This protocol/manuscript has been supported by the Department of Clinical Investigation at Walter Reed Army Medical Center.

In support of their research or preparation of this manuscript, one or more of the authors received grants or outside funding from the Department of Clinical Investigation, Walter Reed Army Medical Center, Work Unit #00-2403. None of the authors received payments or other benefits or a commitment or agreement to provide such benefits from a commercial entity. No commercial entity paid or directed, or agreed to pay or direct, any benefits to any research fund, foundation, educational institution, or other charitable or nonprofit organization with which the authors are affiliated or associated.

References

1. **Aaron RK, Scott R.** Supracondylar fracture of the femur after total knee arthroplasty. *Clin Orthop.* 1987;219:136-9.
2. **Delpont PH, Van Audekercke R, Martens M, Mulier JC.** Conservative treatment of ipsilateral supracondylar femoral fracture after total knee arthroplasty. *J Trauma.* 1984;24:846-9.
3. **Figgie MP, Goldberg VM, Figgie HE 3rd, Sobel M.** The results of treatment of supracondylar fracture above total knee arthroplasty. *J Arthroplasty.* 1990; 5:267-76.
4. **Huo MH, Sculco TP.** Complications in primary total knee arthroplasty. *Orthop Rev.* 1990;19:781-8.
5. **Merkel KD, Johnson EW Jr.** Supracondylar fracture of the femur after total knee arthroplasty. *J Bone Joint Surg Am.* 1986;68:29-43.
6. **Ritter MA, Faris PM, Keating EM.** Anterior femoral notching and ipsilateral supracondylar femur fracture in total knee arthroplasty. *J Arthroplasty.* 1988; 3:185-7.
7. **Webster DA, Murray DG.** Complications of variable axis total knee arthroplasty. *Clin Orthop.* 1985;193:160-7.
8. **Ayers DC.** Supracondylar fracture of the distal femur proximal to a total knee replacement. *Instr Course Lect.* 1997;46:197-203.
9. **Bogoch E, Hastings D, Gross A, Gschwend N.** Supracondylar fractures of the femur adjacent to resurfacing and MacIntosh arthroplasties of the knee in patients with rheumatoid arthritis. *Clin Orthop.* 1988;229:213-20.
10. **Cain PR, Rubash HE, Wissinger HA, McClain EJ.** Periprosthetic femoral fractures following total knee arthroplasty. *Clin Orthop.* 1986;208:205-14.
11. **Cordeiro EN, Costa RC, Carazzato JG, Silva JdosS.** Periprosthetic fractures in patients with total knee arthroplasties. *Clin Orthop.* 1990;252:182-9.
12. **Convery FR, Minter-Convery M, Malcolm LL.** The spherocentric knee: A re-evaluation and modification. *J Bone Joint Surg Am.* 1980;62:320-7.
13. **Culp RW, Schmidt RG, Hanks G, Mak A, Esterhai JL Jr, Heppenstall RB.** Supracondylar fracture of the femur following prosthetic knee arthroplasty. *Clin Orthop.* 1987;222:212-22.
14. **DiGioia AM 3rd, Rubash HE.** Periprosthetic fractures of the femur after total knee arthroplasty. A literature review and treatment algorithm. *Clin Orthop.* 1991;271:135-42.
15. **Hirsh DM, Bhalla S, Roffman M.** Supracondylar fracture of the femur following total knee replacement. Report of four cases. *J Bone Joint Surg Am.* 1981;63:162-3.
16. **Moran MC, Brick GW, Sledge CB, Dysart SH, Chien EP.** Supracondylar femoral fracture following total knee arthroplasty. *Clin Orthop.* 1996;324:196-209.
17. **Sisto DJ, Lachiewicz PF, Insall JN.** Treatment of supracondylar fractures following prosthetic arthroplasty of the knee. *Clin Orthop.* 1985;196:265-72.
18. **Zehntner MK, Ganz R.** Internal fixation of supracondylar fractures after condylar total knee arthroplasty. *Clin Orthop.* 1993;293:219-24.
19. **Healy WL, Siliski JM, Incavo SJ.** Operative treatment of distal femoral fractures proximal to total knee replacements. *J Bone Joint Surg Am.* 1993;75:27-34.
20. **Alho A, Husby T, Høiseth A.** Bone mineral content and mechanical strength. An ex vivo study on human femora at autopsy. *Clin Orthop.* 1988;227:292-7.
21. **Augat P, Reeb H, Claes LE.** Prediction of fracture load at different skeletal sites by geometric properties of the cortical shell. *J Bone Miner Res.* 1996; 11:1356-63.
22. **Cummings SR, Black DM, Nevitt MC, Browner W, Cauley J, Ensrud K, Genant HK, Palermo L, Scott J, Vogt TM.** Bone density at various sites for prediction of hip fractures. The Study of Osteoporotic Fractures Research Group. *Lancet.* 1993;341:72-5.
23. **Heneghan JP, Kirke PN, Murphy BL, Darcy E, Daly L, Bourke GJ, Dinn E, Masterson J.** Evaluation of quantitative CT vertebral bone mineral density measurements and Singh index in elderly females with hip fractures—a case control study. *Br J Radiol.* 1997;70:923-8.
24. **Wachter NJ, Augat P, Mentzel M, Sarkar MR, Krischak GD, Kinzl L, Claes LE.** Predictive value of bone mineral density and morphology determined by peripheral quantitative computed tomography for cancellous bone strength of the proximal femur. *Bone.* 2001;28:133-9.
25. **Wand JS, Hill ID, Reeve J.** Coxarthrosis and femoral neck fracture. *Clin Orthop.* 1992;278:88-94.
26. **Singh M, Nagrath AR, Maini PS.** Changes in trabecular pattern of the upper end of the femur as an index of osteoporosis. *J Bone Joint Surg Am.* 1970; 52:457-67.
27. **Wiss DA.** Supracondylar and intercondylar fractures of the femur. In: Rockwood CA Jr, Green DP, Bucholz RW, Heckman JD, editors. *Rockwood and Green's fractures in adults.* Philadelphia: Lippincott-Raven; 1996. p 1972-94.
28. **Lesh ML, Schneider DJ, Deol G, Davis B, Jacobs CR, Pellegrini VD Jr.** The consequences of anterior femoral notching in total knee arthroplasty. A biomechanical study. *J Bone Joint Surg Am.* 2000;82:1096-101.
29. **Martin RB, Burr DB.** Non-invasive measurement of long bone cross-sectional moment of inertia by photon absorptiometry. *J Biomech.* 1984; 17:195-201.
30. **Masud T, Jawed S, Doyle DV, Spector TD.** A population study of the screening potential of assessment of trabecular pattern of the femoral neck (Singh index): the Chingford Study. *Br J Radiol.* 1995;68:389-93.
31. **Peacock M, Liu G, Carey M, Ambrosius W, Turner CH, Hui S, Johnston CC Jr.** Bone mass and structure at the hip in men and women over the age of 60 years. *Osteoporosis Int.* 1998;8:231-9.
32. **Peacock M, Turner CH, Liu G, Manatunga AK, Timmerman L, Johnston CC Jr.** Better discrimination of hip fracture using bone density, geometry, and architecture. *Osteoporosis Int.* 1995;5:167-73.